# ARDUINO-BASED AUTOMATED SYSTEM FOR SORTING, IDENTIFYING AND GEOREFERENCING SOIL SAMPLES

1

# SISTEM AUTOMATIZAT BAZAT PE ARDUINO PENTRU SORTAREA, IDENTIFICAREA ȘI GEOREFERENȚIEREA PROBELOR DE SOL

## Mario CRISTEA 1), Cristian SORICA1) Robert-Dorin CRISTEA \*1)

1) National Institute of Research - Development for Machines and Installations Designed to Agriculture and Food Industry – INMA Bucharest / Romania

E-mail: robertcri@yahoo.com

DOI: https://doi.org/10.35633/inmateh-77-46

Keywords: automation, prototyping, Arduino, Industrial automation, IoT

## **ABSTRACT**

This article presents the development and experimental validation of an automated module for sorting, identifying, and temporarily storing soil samples, implemented on an Arduino development board. The system was conceived as an auxiliary unit that can be seamlessly integrated into existing soil sampling equipment, automating the post-extraction operations. By directing each sample automatically to a designated container, the module eliminates manual handling, which is labor-intensive and prone to error. Each container is assigned a unique identifier using the PN532 NFC/RFID module, while GPS coordinates, date, and time are simultaneously recorded. Tests performed on a functional prototype demonstrated reliable operation. The carousel mechanism demonstrated performance consistent with functional requirements, the inductive sensors achieved 100% detection accuracy, and the PN532 NFC/RFID module reached a 97% reading success rate. The system ensures full sample traceability, reduces contamination risk, and, by automating critical sorting and labeling steps, significantly enhances the overall efficiency of the analytical workflow.

## **REZUMAT**

Acest articol prezintă dezvoltarea și validarea experimentală a unui modul automat pentru sortarea, identificarea și stocarea temporară a probelor de sol, implementat pe o placă de dezvoltare Arduino. Sistemul a fost conceput ca o unitate auxiliară care poate fi integrată perfect în echipamentele existente de prelevare a probelor de sol, automatizând operațiunile post-extracție. Prin direcționarea automată a fiecărei probe către un recipient desemnat, modulul elimină manipularea manuală, care necesită multă muncă și este predispusă la erori. Fiecărui recipient i se atribuie un identificator unic folosind modulul PN532 NFC/RFID, în timp ce coordonatele GPS, data și ora sunt înregistrate simultan. Testele efectuate pe un prototip funcțional au demonstrat o funcționare fiabilă. Mecanismul carusel a demonstrat performanțe conforme cu cerințele funcționale, senzorii inductivi au atins o precizie de detecție de 100%, iar modulul PN532 NFC/RFID a atins o rată de succes a citirii de 97%. Sistemul asigură trasabilitatea completă a probelor, reduce riscul de contaminare și, prin automatizarea etapelor critice de sortare și etichetare, îmbunătățește semnificativ eficiența generală a fluxului de lucru analitic.

# INTRODUCTION

In the context of the rapid development of technology in agriculture, automation based on the Arduino platform represents an accessible and versatile solution, capable of optimizing agricultural processes and improving the efficiency of operations in this essential sector (*Vinod Chandra S.S. et al., 2024*). Arduino, an open-source platform recognized for its flexibility and ease of programming, offers farmers the opportunity to integrate intelligent systems for monitoring and controlling critical parameters, such as soil moisture, temperature, lighting level or efficient use of resources (*Akshay Y. et al., 2022; José-Antonio M. et al., 2024*).

Over the past two decades, the role of the Internet of Things (IoT) in agriculture has become central to the digitalization of production processes. IoT-based systems provide the necessary infrastructure to connect sensors, drones, and real-time data analysis platforms, allowing farmers to make informed decisions on fertilization, irrigation, and plant disease control (*Ayaz M. et al., 2019*). In a global context marked by decreasing agricultural areas and increasing food pressure, these technologies support the shift from statistical methods to quantitative, precision-oriented approaches.

Studies show that integrating IoT into precision agriculture can reduce water consumption by up to 25% and nutrient losses by over 30%, through adaptive control of irrigation and fertilization (*Ayaz M. et al., 2019*).

The integration of Internet of Things (IoT) technologies with Arduino platforms has fundamentally transformed the way agronomic data is collected and analyzed. Arduino-based smart sensors allow real-time monitoring of soil temperature and moisture, facilitating the implementation of "smart farming" systems that optimize resource consumption and improve productivity (*Nayyar A., Puri V., 2016*). These practical monitoring systems for protected crops demonstrate the ability of accessible platforms to provide viable solutions for modern agriculture (*Morales C. A. H. et al., 2022*).

At the same time, recent advances in electrochemical sensors allow real-time measurement of nitrogen, phosphorus and potassium (NPK) concentrations directly in the soil, using Arduino microcontrollers as data processing and transmission units. Systems based on electrochemical Ion Selective Field Effect Transistors (ISFET) can ensure rapid nutrient detection with response times below 30 seconds, providing a valuable tool for variable fertilization (*Salve A. B. et al., 2018*). These solutions, complemented by wireless sensor networks and automatic calibration algorithms, reduce the costs of laboratory analysis and allow immediate adaptation of fertilizer doses depending on the type of crop and soil texture. In this way, smart sensors supported by Arduino directly contribute to achieving the goals of sustainable agriculture, minimizing losses and the ecological impact of fertilization.

The development of low-cost automated systems has favored the inclusion of Arduino microprocessors in robots or robotic arms, even in small farms that grow vegetables or fruits in a hydroponic system (*Haider A. K. et al., 2024*). In China, a machine for lateral transplanting of sweet potato seedlings on mulch film has been developed, equipped with an Arduino-based controller for coordinated management of system components (*Wanzhi Z. et al., 2024*). In response to climate change and the increasing frequency of droughts, various intelligent automatic irrigation systems have been developed that optimize water consumption (*Salvatore F. G. et al., 2024*).

The versatility of the Arduino microcontroller is also evident in automated sorting applications (*Harshwardhan B. et al., 2023*) and in precision robots designed for the collection and storage of agricultural products. In combination with the Raspberry Pi, Arduino can calculate trajectories for robotic arms towards visually detected targets and control pneumatic systems for object manipulation (*Sharath G.S. et al., 2021*). The performance of a flexible, hydraulically driven robotic arm integrated with an advanced Arduino-based control system - capable of performing multiple functions - has also been demonstrated, including gripping vegetables or fruits, performing small excavations, and suctioning grains from containers (*Yifan C. et al., 2022*). Furthermore, the Arduino microcontroller has been applied in penetrometry, offering advantages in measurement accuracy and enabling the recording of data with temporal and GPS location parameters (*Kumari N. et al., 2023*).

In parallel, research on soilless agriculture has shown that IoT-controlled hydroponic systems based on Arduino microcontrollers can significantly improve the productivity and quality of high-value crops such as saffron, lettuce, and strawberries. A smart hydroponic framework proposed by *Kour et al.* (2022) for saffron cultivation demonstrated that the integration of pH, electrical conductivity, and temperature sensors with automatic nutrient adjustment algorithms enables the continuous maintenance of optimal growth parameters. In these systems, data are transmitted in real time to cloud platforms, where predictive analytics support agronomic decision-making. The results indicated a 35% increase in yield and a 40% reduction in water consumption, confirming the potential of the IoT–Arduino–hydroponics combination for precision crop production (*Kour K. et al., 2022*).

Soil sample collection and analysis are fundamental processes in precision agriculture, providing essential information for nutrient management and optimizing crop yields. Modern sampling strategies, such as grid or zone sampling, enable producers to develop precise prescription maps for variable fertilizer application and soil pH adjustment, thereby improving the accuracy of agricultural input management (*Mylavarapu et al.*, 2020). However, traditional methods of sampling and labeling involve labor-intensive manual procedures that are susceptible to human error, cross-contamination, and inconsistencies in documentation.

Automatic identification technologies such as RFID (Radio-Frequency Identification) and NFC (Near Field Communication) offer innovative solutions for improving traceability in the agri-food supply chain.

RFID systems have demonstrated the ability to ensure complete traceability of fresh agricultural products from the field to the final consumer, significantly improving business processes across the entire supply chain (*Mele F. et al., 2013*). Similarly, NFC technology enables the collection and accumulation of information throughout the entire production process, delivering traceability data directly to the consumer (*Pizzuti T. et al., 2015*). More recently, the integration of blockchain with RFID technology has shown great potential to create secure traceability systems that retain detailed information and ensure the immutability of agricultural product data (*Tian P. et al., 2024*).

Current trends in precision agriculture indicate an accelerated convergence among IoT, robotics, and artificial intelligence, aimed at achieving fully autonomous farms. A recent example is the automated irrigation system proposed by *Abo-Zahhad*, (2023), which integrates Arduino with soil sensors (moisture and pH), light and air humidity sensors, weather forecasts, and machine learning algorithms (KNN) to anticipate crop needs and automatically adjust irrigation. This system has demonstrated significant reductions in water consumption while maintaining optimal conditions for plant development, providing a practical and scalable model for integrating smart technologies into modern farming.

This article presents the development and testing of an automated module for sorting, identifying, and temporarily storing soil samples, based on an Arduino development board. The system is designed as an auxiliary unit that can be easily integrated into existing soil sampling equipment, automating the processes that follow sample extraction. This solution eliminates error-prone manual handling by automatically directing each sample to a predetermined container.

The process involves reading a unique identifier via the PN532 NFC/RFID module and recording the exact GPS coordinates along with the timestamps of sample collection. Tests conducted on a functional prototype confirmed the system's performance: the carousel mechanism operated according to design requirements, the inductive sensors ensured 100% container detection accuracy, and the PN532 NFC/RFID module achieved a 97% success rate in reading. The system guarantees full sample traceability, minimizes contamination risks, and, by automating critical sorting and labeling processes, significantly enhances the efficiency of the analytical workflow.

## **MATERIALS AND METHODS**

# General system architecture

The proposed system consists of a carousel mechanism with sample containers, a control unit based on an Arduino Uno, a PN532 NFC/RFID module, inductive sensors for detecting the position and presence of the containers, and a communication interface integrated into the Arduino board. The general architecture of the system is illustrated in Fig. 1.

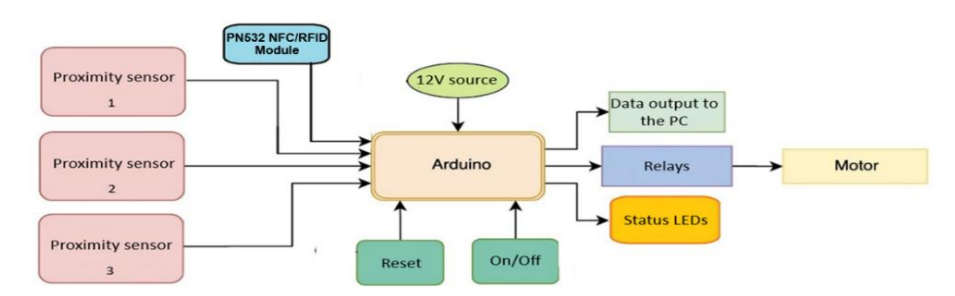


Fig. 1 - Block diagram of the device for sorting, storing and identifying soil samples

The connections to the Arduino are:

# Sensors LJ12A3 (NPN):

- Sensor 1: to digital pin D2 on Arduino.
- Sensor 2: to digital pin D3 on Arduino.
- Sensor 3: to digital pin D4 of Arduino.

# Motor Relay:

- Control pin (IN/SIGNAL): Connects to digital pin D5 on Arduino.
- VCC: Connects to 5V from Arduino.
- GND: Connects to GND from Arduino.

# Motor (12V):

- Connect the positive (+) terminal of the motor to NO (Normally Open).
- Connect the common terminal (COM) of the relay to the positive terminal (+) of the external 12 V battery.
- Connect the negative (-) terminal of the motor to the negative (-) terminal of the external 12 V battery.

## RFID sensor PN532:

- This module uses the SPI protocol.
- VCC: Connects to 5 V from Arduino.
- GND: Connects to GND from Arduino.
- RST (Reset): connected to D 8.
- SCK: Connects to pin D13 on Arduino (SPI Clock).
- MISO: Connects to pin D12 on Arduino (SPI Master In Slave Out).
- MOSI: Connects to pin D11 on Arduino (SPI Master Out Slave In).
- SS (Slave Select) / SSEL: Connects to pin D10 on Arduino (A PN532 RFID library will need to be included).

Figure 2 shows an example of a connection diagram made for this equipment. The input and output connections of the Arduino microcontroller are defined when the program is made using the IDE programming interface. These can also be modified depending on the requirements and the types of sensors and switches used in the creation.

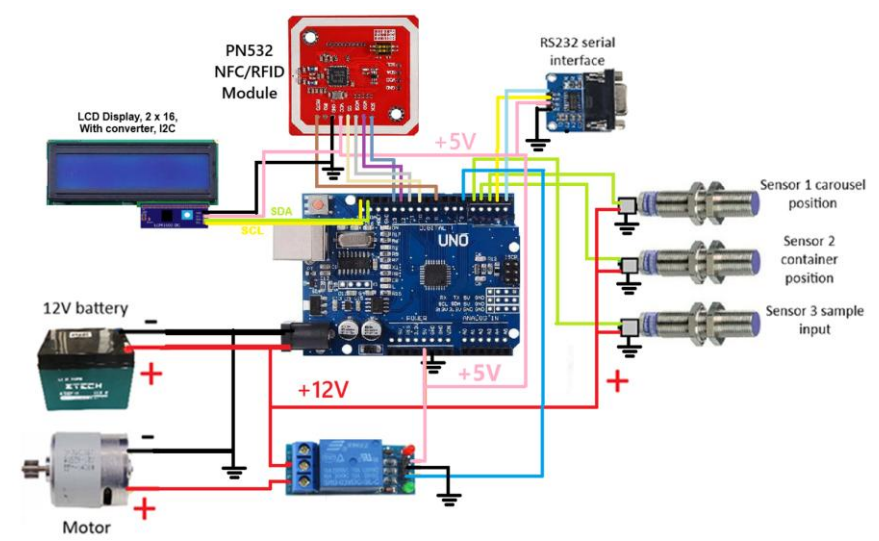


Fig. 2 - Example of sensor connection

## Main hardware components:

## Control unit: Arduino Uno

The core of the control system is the Arduino Uno Rev3 development board, selected as the optimal solution for the prototyping stage due to its low cost, wide availability, extensive user community and rich ecosystem of software libraries and educational resources. The board is built around the ATmega328P microcontroller, whose resources (number of pins, available memory) were sufficient to manage all the required functions: reading three digital sensors, controlling a relay, communicating with the RFID module and transmitting data.

The main technical characteristics of the microcontroller, essential for this project, are: Architecture: 8-bit RISC; Clock speed: 16 MHz; Flash memory: 32 KB (of which 0.5 KB are used by the bootloader); SRAM: 2 KB; EEPROM: 1 KB; Digital I/O pins: 14 (of which 6 can be used as PWM outputs); Analog input pins: 6 (10-bit resolution); Operating voltage: 5 V.

Justification of choice: For this prototyping and concept validation stage, the resources offered by the Arduino Uno and the ATmega328P microcontroller (number of pins, available memory) were sufficient to handle all the required functions: reading three digital sensors, controlling a relay, communicating with the RFID module and transmitting data. The use of the Arduino IDE development environment allowed for a rapid and iterative implementation of the software, which is vital in the concept validation phase under laboratory conditions.

Field Implementation Considerations: Tests have demonstrated the functionality of the system in a controlled environment. However, for practical implementation in real field conditions, where large temperature variations (-10°C to +40°C), high humidity, intense mechanical vibrations, and electromagnetic noise generated by motors and power converters occur, it is necessary to move to industrial-grade platforms. Recommended options include:

- Arduino Opta: An IP66-rated micro-PLC, specifically designed for industrial automation and harsh environments:
- Arduino Mega 2560: For applications requiring a larger number of sensors or extended functionality;
- ARM microcontroller-based solutions: For applications requiring higher processing power and faster communication speeds;

The use of the Arduino IDE development environment allowed for rapid and iterative implementation of the software, which was essential in the proof of concept phase. However, for applications in field conditions, characterized by large variations in temperature, humidity and electromagnetic noise, it is recommended to switch to more robust platforms, such as the Arduino Opta (a micro-PLC with IP66 protection), the Arduino Mega 2560 or solutions based on ARM microcontrollers. The choice of the Arduino Uno was therefore justified for the demonstration purpose of the prototype, with a mention of the future transition to industrial components.

## Container position and presence sensors

Three LJ12A3-4-Z/BX inductive proximity sensors were used to detect the carousel position and the presence of containers (Figure 3). They were selected due to their immunity to dust, dirt and moisture, as well as the advantage of non-contact detection, which reduces mechanical wear. Within the system, two sensors are dedicated to identifying the "zero" position and the passage of containers, and the third is responsible for detecting the introduction of the sample. This configuration ensures reliable synchronization of the carousel rotation and a precise correlation with the container filling process.



Fig. 3 - Inductive proximity sensor - LJ12A3

The operating principle is based on electromagnetic induction; the sensor detects the presence of metal objects. Main technical specifications: supply voltage: 6-36 V DC, output current: ≤300 mA, switching distance: 4 mm (±10%), switching frequency: 100 Hz. Two sensors are used to detect the "zero" position of the carousel and the passage of containers, and one to detect the entry of the sample into the system.

## Motion drive and control system

The carousel is driven by a DC electric motor (12 V, 4.5 A) with an integrated reducer, which provides sufficient torque to rotate the load.

The motor control (on/off) is done by a single-channel, galvanically isolated relay, which switches the motor power supply on command from a digital pin of the Arduino. The choice of a relay instead of a motor driver (e.g. H-bridge) is justified by the simplicity of the requirements (only on/off in one direction) and the low cost.

The motor that drives the carousel is a 12 V powered motor. Motor specifications: Supply voltage 12 V; Nominal power: 20.7 W; Nominal current: 4.5 A; Nominal speed: 44 rpm; Nominal torque: 4.5 Nm.

# The system of identification of samples

To uniquely identify each container, the system uses a PN532 RFID Module (figure 4).



Fig. 4 - RFID module PN532

It was chosen due to its ability to detect the presence of RFID identifiers with high accuracy and its high resistance to dust.

## Specifications:

- Working frequency: 13.56 MHz;
- o Supported cards: Mifare 1k, 4k, Ultralight, and DesFire; ISO/IEC 14443-4: CD97BX, CD light, Desfire, P5CN072 (SMX); Jewel (IRT5001); FeliCa (RCS\_860 or RCS\_854);
- o PCB antenna with 4-6 cm communication distance;
- I2C, UART, SPI interfaces selectable via switches 00=UART, 10=I2C, 01=SPI.

# Power and communication system

The system is powered by an external 12 V battery. The 5V voltage is controlled by the Arduino for the modules that are powered by this voltage. The data (container ID, timestamp, GPS coordinates) are transmitted to an external computer using the RS232 protocol, via a USB-to-TTL adapter module (such as those based on the FT232RL or CH340 chipsets), connected to the dedicated pins of the Arduino, configured as a SoftwareSerial interface.

# Testing procedures.

The prototype was tested in a laboratory environment. It was evaluated:

- Motor performance: Carousel angular velocity and current consumption.
- **Sensor reliability**: Number of correct container detections per 100 cycles; RFID detection success rate expressed as the number of successful reads per 100 attempts.
- **Positioning accuracy**: Angular and linear error measured over 100 consecutive complete rotations (360°), stopping at the same reference position. Measurements were performed for both empty containers (n=50) and containers filled with soil (n=50). For each stop, the linear deviation from the reference point was measured using a digital caliper with a resolution of 0.01 mm. The angular error was calculated based on the measured linear error and the radius of the carousel.

## Data flow and communication architecture

The system implements an edge computing architecture, where the Arduino board functions as an edge node responsible for process control and data generation. At the end of each container filling cycle, the microcontroller generates a digital register that includes the container ID (read via RFID), GPS coordinates and sampling timestamp. This data is transmitted via the RS232 serial interface to a higher-level gateway unit (PC or Raspberry Pi), which can then ensure transmission to cloud platforms via GSM/4G connection (figure 5).

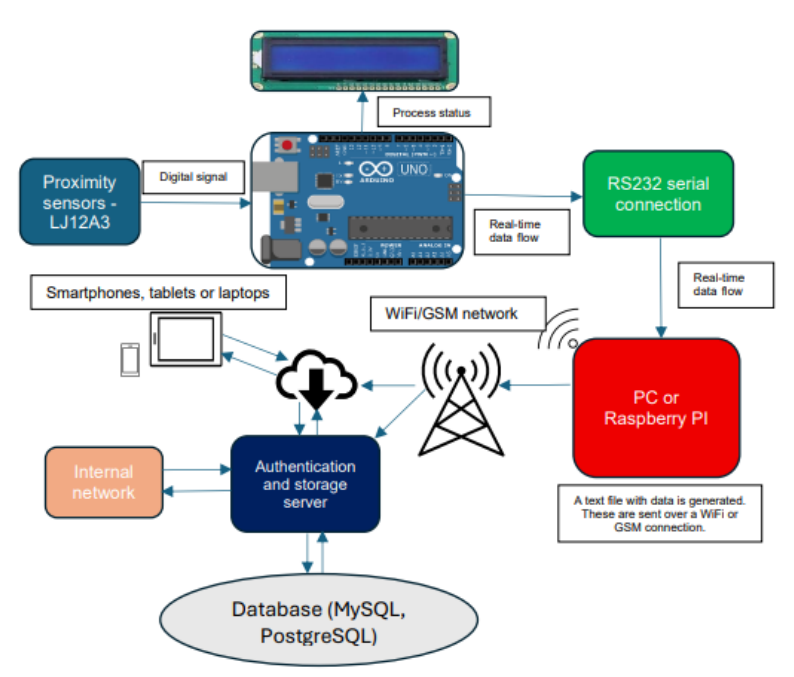


Fig. 5 - Data flow diagram from the Arduino to the end user.

Note: The complete implementation of the cloud communication infrastructure (security protocols, authentication, latency, databases) is beyond the scope of this article, which focuses on the functional

validation of the sorting and identification module. This data architecture will be detailed in a future paper dedicated to the integration of the system into agricultural IoT platforms.

**Justification:** This two-tier architecture (edge + gateway) is optimal in terms of reliability and cost. The Arduino, with its limited resources, is only responsible for critical real-time tasks (control, data generation). The computationally intensive task of communicating with the cloud is delegated to a gateway with more resources (Raspberry Pi, PC) and a dedicated network connection, ensuring that the basic operation of the field system is not affected by possible GSM connectivity issues.

## **RESULTS AND DISCUSSION**

# **Motor performance**

The motor performance data is presented in Table 1. The results show a linear relationship between the supply voltage and the speed at the output of the reducer, which was expected for a DC motor.

Table 1: Carousel drive motor performance.

Table 1

Voltage (V)	Current (A)	Power consum ed (W)	Rotation at the output of the shaft from the worm gear (rpm)	Carousel speed (rad/s)
9.20	2.40	22.08	15.96	1.67
9.90	2.49	24.65	19.45	2.04
11.10	2.63	29.19	25.49	2.67
12.00	2.71	32.52	28.86	3.02
12.50	2.73	34.13	32.36	3.39
13.00	2.76	35.88	35.31	3.70
14.50	2.85	41.33	41.88	4.39
15.00	2.86	42.90	45.16	4.73
15.50	2.89	44.80	48.99	5.13
16.00	2.91	46.56	50.50	5.29

The angular velocity of the carousel, calculated according to the relationship:

$$\omega = \frac{2\pi n}{60} \text{ [rad/s]} \tag{1}$$

where  $\omega$  is the angular velocity for the voltage range tested, in rad/s, n is the speed at the output of the worm gear shaft in s<sup>-1</sup>.

The power consumed was calculated with the relationship:

$$P = VI [W] (2)$$

where P is the power consumed, [W], V is the supply voltage, [V], I is the intensity of the electric current, [A].

Based on these data, for stable operation and adequate response time, the optimal working voltage was set at 12 V. At this voltage, the angular velocity of the carousel is 3.02 rad/s. This speed is compatible with the working speed of most manual or semi-automatic sampling machines. The quasi-linear increase in speed confirms the predictable behavior of the DC motor and worm gear, which facilitates precise control of the positioning of soil sample containers.

The total system power consumption ranged from 22 W at 9.2 V to 46.6 W at 16 V. Based on the specifications of the 12 V-7 Ah (84 Wh) battery and the analytical determination of the system power consumption rate, the designed autonomy was set at approximately 2.5 hours of continuous operation.

The analysis of the operating regime of the electric motor indicates a quasi-linear correlation between the consumed power and the applied voltage, a typical behavior for a system operating in its linear direct current (DC) range. It was observed that, as the supply voltage increases, the absorbed current maintains a remarkable stability, fluctuating in a narrow range of 2.4 A to 2.91 A.

This current constancy suggests that the load applied to the motor is predominantly of a restrictive mechanical nature, limiting the electrical variations, and not the result of internal constraints of an electrical or thermal nature. Therefore, it can be concluded that the motor does not reach saturation or overheating limits.

A complete assessment of the energy efficiency of the system requires the quantification of the mechanical power effectively delivered to the carousel shaft (axis), thus allowing the determination of the ratio between the useful mechanical power and the total electrical power consumed.

The carousel speed increases proportionally to the voltage, suggesting that friction and mechanical losses are relatively constant over the operating range (9–16 V). If a concave curve towards saturation were observed, it would indicate torque limitation or variable friction. But from the current table, the increase is almost linear, so the worm gear is operating efficiently.

After determining the rotation speed, the time required for a complete rotation of the carousel can be calculated:

$$T_{max} = \frac{2\pi}{\omega} [s] \tag{3}$$

where  $T_{max}$  is the maximum time in which a complete rotation of the carousel takes place, [s].

Also using this relationship, the time required to index each container can be calculated. Calculating the rotation time for a step:

$$t_s = \frac{\Delta\theta}{\omega} = \frac{\pi/6}{3.02} \approx 0.174 \, s \tag{4}$$

where  $t_s$  is the time required for a single step, [s];  $\Delta\theta$  is the rotation angle required to move a container from its current position to the next carousel position, [rad].

The pure rotation time required to index a container from one position to the next is only a partial component of the total operational cycle. In practice, other dynamic and stationary phases are also integrated to obtain a realistic estimate of the system performance. These additional phases include: the acceleration and deceleration profile of the carousel, which is essential for managing inertia, minimizing mechanical shocks and preventing load slippage; this step can lead to a doubling of the pure rotation time, adding approximately 0.35 s to the cycle. Additionally, a time interval of 0.2–0.3 s must be allocated for the precise stabilization of the carousel at the final position, thus allowing the execution of critical operations (e.g. reliable reading of RFID tags or other interventions). The final estimate of the operational time per container, under 12 V operating conditions, is thus in the range of 0.35–0.5 s, reflecting a holistic understanding of the motion dynamics and precision requirements.

Time per step  $t_s$  is inversely proportional to angular velocity (angular velocity as a function of voltage):

$$t_{s} = \frac{\Delta \theta}{\omega (U)} [s] \tag{5}$$

Because the angular velocity  $(\omega)$  is, in turn, a function of the supply voltage  $(\mathit{U})$ , this interdependence allows drawing a voltage regulation curve  $(\mathit{U})$  which can be used to optimize cyclic performance. By fine-tuning the voltage, the system can achieve an optimal operating time that achieves a functional balance between the speed of indexing and the accuracy requirement needed to complete stationary operations under maximum stability conditions.

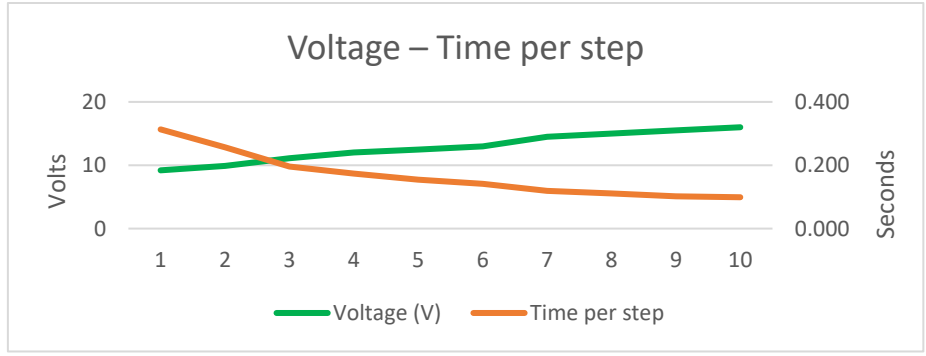


Fig. 6 - Graph "Voltage - Time per step"

The graph in figure 6 illustrates the variation of the time to position a container as a function of the motor supply voltage. It is observed a significant and almost inversely proportional decrease in the time required to move the carousel by one step (30°) as the voltage increases.

At low voltages (9.2 V), the positioning time is approximately 0.31 s, which indicates a low angular velocity of the system ( $\approx$  1.67 rad/s). At values close to 16 V, the time drops below 0.1 s, corresponding to a velocity of  $\approx$  5.3 rad/s. This variation highlights the sensitivity of the motor to the power supply and confirms that by adjusting the input voltage, the rotation speed of the carousel can be precisely controlled.

The shape of the curve is monotonically decreasing and slightly nonlinear, which is specific to DC electric motors with constant mechanical load, where increasing the voltage causes both an increase in speed and a slight increase in current and, implicitly, in the power consumed.

From a practical point of view, these results allow choosing a compromise between operating time (speed) and positioning stability. At high voltages, although the time per step drops below 0.1 s, vibrations and stopping errors can occur due to inertia. At moderate voltages (12–13 V), the time of  $\approx$  0.15–0.17 s/step provides a sufficiently high speed, but also better stability at stopping.

The quasi-linear relationship observed between the angular velocity of the system and the supply voltage (modulated by PWM control from the Arduino platform) indicates a high degree of predictability in the command-control system. This behavior facilitates the implementation of precise positioning strategies for active elements, such as containers. In the context of operational requirements, achieving high angular velocities (e.g., 5.29 rad/s) optimizes the indexing time, resulting in a very fast rotation cycle (≈1.2 s/rotation). However, this speed imposes the need to introduce acceleration/deceleration profiles to ensure reliable reading of RFID tags and to mitigate potential structural vibrations. In contrast, operating at low angular velocities (e.g., ≈1.67 rad/s) improves mechanical stability and stopping accuracy, but correspondingly extends the time required to complete an experimental cycle, thus affecting the processing throughput.

The container positioning error, essentially defined as the stopping accuracy of the system, is an intrinsic characteristic determined by the performance of the control system (consisting of a DC motor and a proximity sensor) and not by operational parameters such as the number of revolutions or the weight of the disc, within reasonable limits. This error is generated by a set of factors, mainly intrinsic to the system configuration. First, the accuracy of the inductive proximity sensor (model LJ12A3) is limited by a certain hysteresis zone and a finite repeatability of the switching point, estimated at  $\pm 0.05 - 0.1$  mm from its nominal detection distance of 4 mm. Then, the angular play inherent in the worm mechanism introduces a position error at the disc level, due to the mechanical play between the screw and the wheel. Also, the considerable inertia of the system causes overtravel after the motor power is disconnected, and finally, the reaction time of the control loop – the interval between detecting the proximity signal and the actual stopping of the motor – directly influences the final positioning accuracy.

# Sensor reliability

The carousel mechanism demonstrated performance consistent with the functional requirements: angular velocity of 3.02 rad/s at 12 V operating voltage (according to Table 1), positioning error below 0.6°, and completion of a full sorting cycle in approximately 4.5 seconds. During the 100 test cycles, no jams or mechanical failures were recorded.

The tests performed indicated a high reliability of the inductive sensors, with a detection rate of 100% over 100 cycles. Both the "zero" position sensor and the container detection sensor recorded a 100% success rate (100/100 correct detections). This is due to the robust nature of the inductive sensors and the short operating distance.

The second factor, repeatability error, is determined by sensor performance and system inertia.

To ensure robust detection of containers on the carousel and guarantee 100% recorded accuracy, it was essential to understand and integrate the hysteresis characteristic of the LJ12A3 inductive sensor. The sensor's hysteresis defines the difference between the distance at which it activates (the operating point) and the,  $S_0$ ) and the distance at which it deactivates (the release point,  $S_r$ ). Specifically, for the model used, the hysteresis typically varies between 3% and 15% of the nominal sensing distance. ( $S_n$  =4 mm). This interval (a "dead zone" or band of uncertainty) is crucial.

$$H = |S_o - S_r| \tag{6}$$

where: H is the Hysteresis, [mm];  $S_0$  is the operating point;  $S_r$  is the release point.

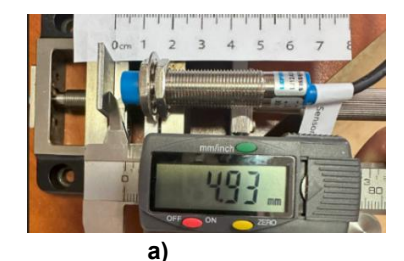
In the data sheet, the hysteresis may be expressed as a percentage of the nominal sensing distance  $(S_n)$ . This percentage value indicates the relative stability of the sensor:

$$H\% = \frac{|S_0 - S_r|}{S_n} X100 \tag{7}$$

where: H% is the relative hysteresis in percent;  $S_n$  is the nominal detection distance of the sensor in mm.

This was exploited in the microcontroller programming to prevent the phenomenon of false switching ("chattering"). Hysteresis acts as a mechanical digital filter, ensuring that a small distance variation caused by the inherent vibrations of the agricultural machinery or the inertia when the engine is stopped does not lead to premature deactivation of the sensor. Thus, by physically positioning the sensor and the metal target, it was guaranteed that once the container is detected and the movement stops, the sensor remains stably activated throughout the NFC/RFID reading process, confirming a firm electrical contact and a correct position for the next operational step.

To determine the distance at which the inductive sensor is activated, a device was used that allows very fine movement in the horizontal plane (figure 7).



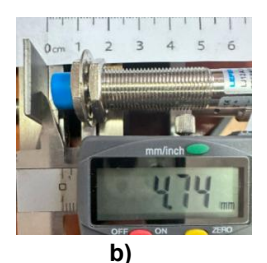


Fig 7 – Checking the activation distance of the inductive sensor: a) distance at which the sensor is inactive, b) distance at which the sensor was activated

By positioning the sensor in the hysteresis zone, it is ensured that minor mechanical fluctuations do not cause a false switching of the sensor, thus ensuring that the "detected" state remains stable throughout the entire duration of the container's parking.

The mass of the carousel without containers is 9.1 kg, the empty container weighs 675 g. After the containers were filled with soil they weighed on average 1580 g. Although the total mass of the system increases from 17.2 kg (carousel weight and empty containers) to approximately 28.00 kg (carousel weight and full containers), leading to higher inertia and potential overtravel, the difference in positioning error is minor in a well-tuned system (figure 8). The direct contribution of the proximity sensor (LJ12A3) is small, since a linear repeatability of 0.05 mm translates into a negligible angular error by calculation.

In conclusion, the positioning error is dominated by the mechanical play, which is constant, and the influence of the weight on the overtravel is marginal. Based on 100 consecutive measurements (full 360° rotations with stopping at the same reference position), the total angular error measured was between 0.1° and 0.6° (mean: 0.35°±0.15°, n=100). This error is constant for each stop, because the system, being a feedback one, does not accumulate the error. In linear terms, this translates to a measured error of approximately 1.0 mm for empty containers (n=50 measurements) and 1.5 mm for full containers (n=50 measurements), the difference being attributed to the increased inertia.



Fig. 8 - Images from container positioning error measurements (n=100 complete rotations) a) empty container (average error 1.0±0.3 mm); b) full container (average error 1.5±0.4 mm)

The PN532 RFID module also performed reliably, recording a 97% read success rate (97/100 attempts).

The success rate in reading NFC/RFID tags was 97%, indicating high operational reliability. The experiments revealed a reading error rate of 3%, the etiology of which is multifactorial, and the specific components could not be experimentally isolated in the current testing phase, imposing a series of fundamental hypotheses: the presence of electromagnetic interference (IEM), likely to be generated by adjacent electrical equipment and affect the 13.56 MHz ISM band used by NFC, although the environment has not been EM mapped, is postulated; a second hypothesis concerns positional dynamics, where micro-vibrations at standstill can alter the angle of incidence of the electromagnetic field, reducing the essential inductive coupling.

In addition, protocol level anomalies, such as transient synchronization errors or CRC failures, are also taken into account. Given that the current study is limited by the absence of direct EM field measurements, empirical validation of these hypotheses requires spectral analyses, Faraday Cage testing, and Signal-to-Noise Ratio (SNR) monitoring, steps necessary in the industrialization phase.

The tag used is not intended to be used on metal surfaces, therefore when using metal surfaces on which RFID tags must be mounted, it is necessary to use tags that have the mention "On-Metal Tags" or "Anti-Metal Tags", for example NXP NTAG213 / NTAG215 / NTAG216.

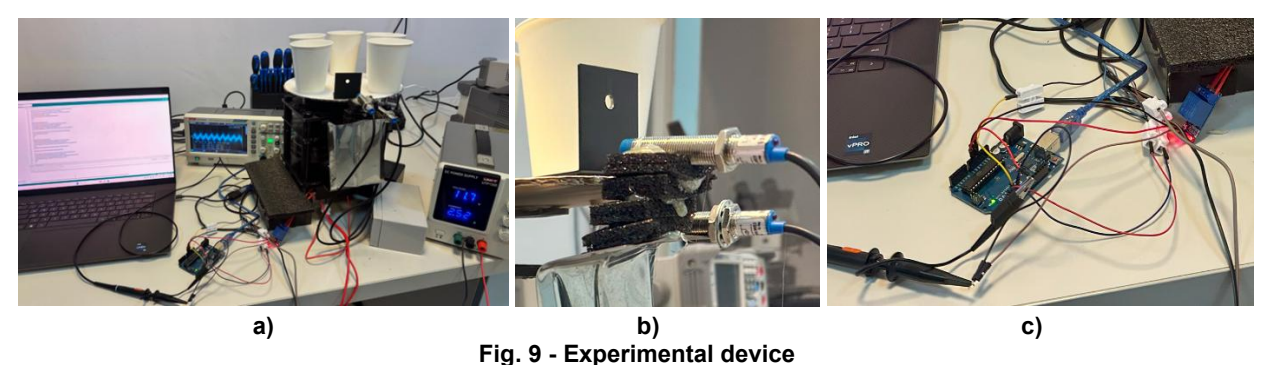
Mitigation measures for the 3% read errors in the industrialization phase can be achieved through both software and hardware optimizations. At the software level, it is recommended to implement an automatic retry algorithm that performs two immediate attempts to read the NFC/RFID tag in the event of an initial failure, before classifying the event as a critical error. At the hardware level, to reduce the influence of electromagnetic interference from the agricultural environment, additional shielding (such as an aluminum housing or Faraday shield) can be used around the PN532 module. These integrated solutions would increase the reliability of the system at the industrial level, ensuring a success rate close to 100%.

To assess the robustness of the results, confidence intervals (95%) were calculated for the tests performed. The success rate of the inductive sensors (100/100) corresponds to an estimated confidence interval of 96.4–100%, which confirms their high reliability. For the PN532 module, the success rate of 97% (97/100) falls within a range of 91.5–99.4%, indicating a consistent performance, with errors occurring as a result of the factors discussed above.

# Experimental setup and prototype validation

To verify the functionality of the entire system and validate the data presented above, a small-scale prototype of the device was built and tested. It included all the essential components: the Arduino Uno board, the inductive sensors, the relay module, the drive motor and the container carousel.

The experimental setup, illustrated in Figure 9, was integrated on a laboratory stand (or adjusted test stand). This setup allowed the tests to be carried out under strictly controlled conditions, essential for rigorous validation of the functionality and correctness of the system's operational sequences. The testing confirmed that the program logic and the interaction between all components work according to the functional requirements, and the data flow is generated and transmitted correctly.



a) general view of the assembly; b) details regarding the mounting of inductive sensors; c) connection interface of the Arduino board and the computer for monitoring

Through this experimental model, it was possible to validate not only the individual performance of the components, but also their integration into a coherent system. This experiment served as a proof of concept before a possible construction of a functional model.

After the operating program and the system logic were validated, without integrating the container identification part, the system was mounted on the device specially built for mounting on soil sampling equipment. The assembly was completed with a display that displays the program status in real time Fig.10.

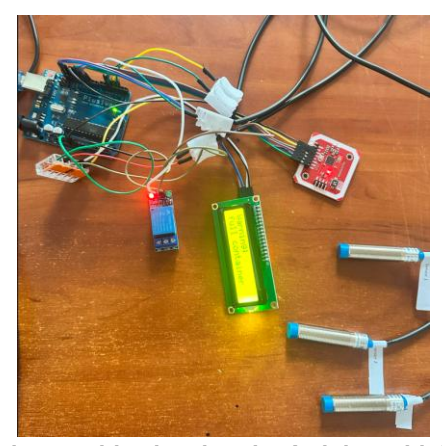


Fig. 10 - Completed assembly showing the Arduino with inductive sensors, RFID module, display, and motor control relay.

On the back of the carousel, 12 +1 pieces of metal measuring 20x20 mm were mounted to activate the inductive sensors and also to power the electric motor used to rotate the carousel (figure 11).

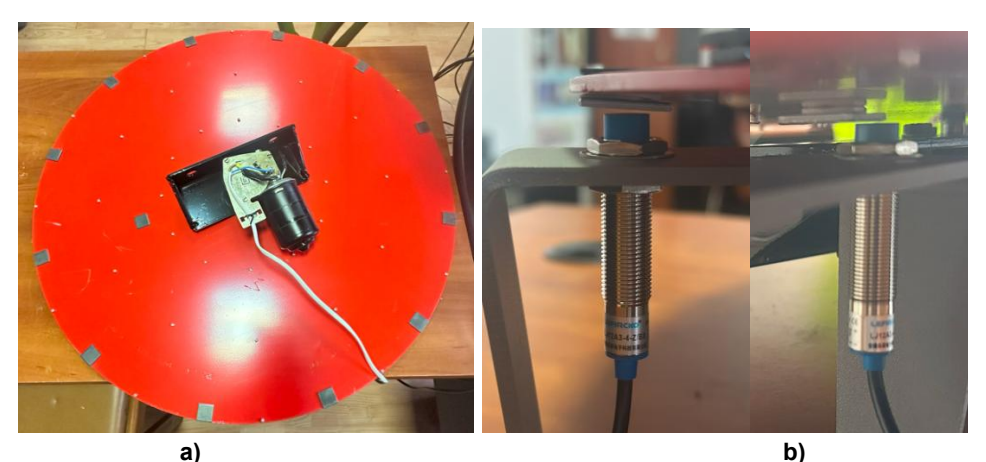


Fig. 11 - Details regarding the installation of inductive sensor activation plates:
a) the location of the metal plates, b) the position of the position sensors

## Limitation

The main limitations of the prototype include sensitivity to the influence of metal surfaces and electromagnetic interference that can disrupt the reception of the RFID sensor and the lack of IP protection against dust and moisture. For a practical implementation, the use of an extended field RFID antenna, tags intended for use on metal surfaces and housings with an IP67 protection rating is recommended.

# **Future perspectives**

Future directions of research include:

- testing in real field conditions and evaluating behavior against vibrations, dust and humidity;
- replacing the tags and Arduino Uno board with an industrial solution (e.g. Arduino Opta or dedicated PLC);
- integration with additional sensors (humidity, temperature, pH) to enrich the metadata associated with each sample.

## **CONCLUSIONS**

In this paper, the successful development, testing and validation of a modular automated system for sorting, labeling and data management of soil samples, built around the Arduino Uno development board, was demonstrated. The paper achieved its main goal of proving the feasibility of a concept for automating the critical post-sampling stage, with a functional validation under laboratory conditions. From an engineering point of view, the prototype demonstrated high operational performance: the selected DC motor operated according to the power analysis performed, and the inductive sensors recorded 100% accuracy in container detection.

This accuracy was supported by the integration of the sensor hysteresis effect in the control logic, preventing the chattering phenomenon caused by vibrations. The NFC/RFID module achieved a 97% success rate in reading tags, and the 3% of errors were analyzed and attributed mainly to transient electromagnetic interference and data transfer, with mitigation solutions proposed (software retry and hardware shielding) for the industrialization phase. The established operating speed (a complete cycle in ~4.5 seconds) is compatible with the working pace of a sampling machine. By eliminating manual handling, the system significantly reduces human errors and the risk of contamination. In conclusion, the implemented robust communication architecture ensures full and real-time traceability of samples, establishing a viable and cost-effective technical framework for improving soil sample management in precision agriculture.

## **ACKNOWLEDGEMENT**

This work was supported by the National Research Authority, through the Project entitled: "An intelligent automated system designed for georeferenced soil sampling." -- PN 23 04 01 02. Contract no./date 9N/ 01.01.2023.

## **REFERENCES**

- [1] Abo-Zahhad, M. M., (2023). IoT-Based Automated Management Irrigation System Using Soil Moisture Data and Weather Forecasting Adopting Machine Learning Technique. *Sohag Engineering Journal, 3*(2), 122-140. https://doi.org/10.21608/sej.2023.209528.1037.
- [2] Akshay Y., Nilesh S. (2023). Development of low-cost data logger system for capturing transmission parameters of two-wheeler using Arduino. *Materials Today: Proceedings*, Volume 72, Part 3, pp 1697-1703, ISSN 2214-7853, https://doi.org/10.1016/j.matpr.2022.09.471.
- [3] Ayaz, M., Ammad-Uddin, M., Sharif, Z., Mansour, A., & Aggoune, E. H. M. (2019). *Internet-of-Things* (*IoT)-Based Smart Agriculture: Toward Making the Fields Talk*. IEEE Access, 7, 129551–129583. https://doi.org/10.1109/ACCESS.2019.2932609
- [4] Fauziah N., Fitriantin N. B., Fakhrurrja H., Simarmata T. (2024). Enhancing soil nutritional status in smart farming: The role of IoT-based management for meeting plant requirements. *International Journal of Agronomy*, 2024, article ID 8874325, 23 pages. https://doi.org/10.1155/2024/8874325.
- [5] Haider A. K., Umar F., Shoaib R. S., Ubaid-ur R., Muhammad N. T., Tahir I., Muhammad Jehanzeb M. C., Muhammad A. A., Saddam H. (2024). Design and development of machine vision robotic arm for vegetable crops in hydroponics. *Smart Agricultural Technology*, Volume 9, 2024, 100628, ISSN 2772-3755, https://doi.org/10.1016/j.atech.2024.100628.
- [6] Harshwardhan B., Shubham D., Hrishikesh S., Piyush G., Shriyash S. (2023). Design and development of bottle sorting machine using Arduino. *Materials Today: Proceedings*, Volume 77, Part 3, 2023, pp 1023-1027, ISSN 2214-7853, https://doi.org/10.1016/j.matpr.2023.02.252.
- [7] José-Antonio M. M., Pedro Antonio G. T., Pablo D. T. (2024). Computational thinking and programming with Arduino in education: A systematic review for secondary education. *Heliyon,* Volume 10, Issue 8, 2024, e29177, ISSN 2405-8440, https://doi.org/10.1016/j.heliyon.2024.e29177.
- [8] Kour, K., Gupta, D., Gupta, K., Dhiman, G., Juneja, S., Viriyasitavat, W., Mohafez, H., & Islam, M. A. (2022). Smart-Hydroponic-Based Framework for Saffron Cultivation: A Precision Smart Agriculture Perspective. *Sustainability*, 14(3), 1120. https://doi.org/10.3390/su14031120
- [9] Kumari N., Ganesh U., Naresh, B. P., Swapnil C., Vijaya R. (2023). A tractor hydraulic assisted embedded microprocessor-based penetrometer for soil compaction measurement. *Journal of Terramechanics*, Volume 110, 2023, pp 1-12, ISSN 0022-4898, https://doi.org/10.1016/j.jterra.2023.07.003.
- [10] Mele F., Patrono L., Simone F., Stefanizzi M. L., Vergallo R. (2013). An RFID-based tracing and tracking system for the fresh vegetables supply chain. *International Journal of Antennas and Propagation*, 2013. https://doi.org/10.1155/2013/531364.
- [11] Morales C. A. H., Luna-Riviera J.M., Perez-Jlmenez R. (2022). Design and deployment of a practical loT-based monitoring system for protected cultivations. *Computer Communications*, 186(3). DOI:10.1016/j.comcom.2022.01.009
- [12] Mylavarapu R., Lee W. S. D. (2020). UF/IFAS nutrient management series: Soil sampling strategies for precision agriculture. *EDIS*, 2020(4). https://doi.org/10.32473/edis-ss402-2020

- [13] Nayyar A., Puri V. (2016). Smart farming: IoT based smart sensors agriculture stick for live temperature and moisture monitoring using Arduino, cloud computing & solar technology. *Proceedings of the International Conference on Communication and Computing Systems*, pp 673–680.
- [14] Pizzuti T., Pigini D., Conti M. (2017). NFC-based traceability in the food chain. *Sustainability*, 9(10), 1910. https://doi.org/10.3390/su9101910.
- [15] Salvatore F. G., Davide C., Andrea B., Alessandro M. (2024). Development of a low-cost smart irrigation system for sustainable water management in the Mediterranean region. *Smart Agricultural Technology*, Volume 9, 2024, 100629, ISSN 2772-3755, https://doi.org/10.1016/j.atech.2024.100629.
- [16] Salve, A. B., Sagar, S. S., Patne, M. L., & Jangam, O. R. (2018). Soil Nutrient Identification Using Arduino and Electrochemical Sensor. International Research Journal of Engineering and Technology (IRJET), 5(2), 1327–1329.
- [17] Sharath G.S., Hiremath N., Manjunatha G. (2021). Design and analysis of gantry robot for pick and place mechanism with Arduino Mega 2560 microcontroller and processed using pythons. *Materials Today: Proceedings*, Volume 45, Part 1, 2021, pp 377-384, ISSN 2214-7853, https://doi.org/10.1016/j.matpr.2020.11.965.
- [18] Tian P., Dai J., Miao F. (2024). Design of agricultural product traceability system based on blockchain and RFID. *Scientific Reports*, 14, 23599. https://doi.org/10.1038/s41598-024-73711-2
- [19] Vinod Chandra S.S., Anand H. S., Ghassan F. A. (2024). Precision farming for sustainability: An agricultural intelligence model. *Computers and Electronics in Agriculture*, Volume 226, 2024, 109386, ISSN 0168-1699, https://doi.org/10.1016/j.compag.2024.109386.
- [20] Wanzhi Z., Qian Z., Tingting Z., Hongjuan L., Guizhi M. (2024). Design and control of a side dense transplanting machine for sweet potato seedlings on mulch film. *Computers and Electronics in Agriculture*, Volume 224, 2024, 109193, ISSN 0168-1699, https://doi.org/10.1016/j.compag.2024.109193.
- [21] Yifan C., Xu S., Haocun W., Meijie H., Fangshu G., (2022). Design of an efficient automated grain unloader based on Arduino. IEEE 6th advanced information technology, electronic and automation control conference (IAEAC). IEEE, ISBN:978-1-6654-5864-1, pp. 1004-1007. DOI: 10.1109/IAEAC54830.2022.9929779.